Available online at www.sciencedirect.com

ScienceDirect

Current Opinion in Structural Biology

Toward a unifying mechanistic model of eukaryotic translation initiation through integrative single-molecule, structural, and computational insights

Brennan Ashwood[1], Victoria Stalls[2] and Ruben L. Gonzalez Jr. [1,3]

During eukaryotic translation initiation, initiation factor proteins and the ribosomal small subunit undergo binding and dissociation reactions and conformational rearrangements that properly assemble a ribosome at the start codon of a messenger RNA. Building on extensive genetic and biochemical studies, single-molecule fluorescence experiments are revealing the time-dependent pathways of factor binding to, and dissociation from, the ribosomal small subunit and messenger RNA during initiation. Nonetheless, essential binding and/or dissociation events, conformational rearrangements, and the coupling between binding and conformational changes remain kinetically uncharacterized. Here, we summarize the status of single-molecule investigations of initiation and advocate for integrating single-molecule microscopy, structural biology, and molecular simulations to enable a time-dependent, molecular description of this fundamental step in gene expression.

Addresses
[1] Department of Chemistry, New York, NY, USA
[2] Department of Biological Sciences, New York, NY, USA
[3] Department of Physiology & Cellular Biophysics, Columbia University, New York, NY, USA

Corresponding author: Gonzalez, Ruben L. (rlg2118@columbia.edu)

Current Opinion in Structural Biology 2026, **98**:103246

This review comes from a themed issue on **Single Molecule and Macromolecular Dynamics (2026)**

Edited by **Mark Bowen** and **Hugo Sanabria**

For a complete overview see the Issue and the Editorial

Available online xxx

https://doi.org/10.1016/j.sbi.2026.103246

Introduction

Translation initiation is a multistep process that serves as the primary mechanism for regulating protein synthesis in response to time-dependent cellular conditions. In eukaryotes, such regulatory capacity is achieved through a series of coordinated binding events and conformational changes between the ribosomal small (40S) subunit, initiator transfer RNA (Met-tRNA$_i$), and numerous eukaryotic initiation factor (eIF) proteins that coordinate the assembly of an elongation-component ribosome at the proper start codon of the messenger RNA (mRNA). Figure 1 illustrates a minimal mechanism for the canonical initiation process, which involves (i) binding of the heterotrimeric eIF4F complex (composed of eIF4G, eIF4E, and eIF4A) to the 5′ 7-methylguanosine 'cap' of the mRNA, which helps (ii) load an eIF- and 40S subunit-containing ribosomal pre-initiation complex (PIC) onto the mRNA. Next, (iii) the PIC searches along the mRNA for the start codon and, upon identifying it, undergoes a series of compositional and conformational changes that (iv) properly select and position the start codon within the PIC and (v) facilitate joining of the ribosomal large (60S) subunit.

Molecular descriptions of the steps in eukaryotic translation initiation remain coarse, but recent genetic, biochemical, and technical advances have created an opening to study this mechanism in unprecedented molecular detail. The key factors of the process have been identified, the phenotypes associated with impairing the functions of many of these factors have been extensively characterized *in vivo* in the yeast *Saccharomyces cerevisiae* [1,2], and translation initiation has been reconstituted *in vitro* with yeast and mammalian systems [3–5]. The detailed genetic and biochemical characterization of eukaryotic translation initiation that these developments have enabled is reviewed elsewhere [1,2,6,7]. In parallel, technical improvements in single-molecule fluorescence microscopy are allowing for increases in the background concentrations of fluorophore-labeled components at which high signal-to-background imaging can be conducted, increases in the number of fluorophore-labeled components that can be simultaneously visualized, and the time resolution with which their activities can be monitored, allowing for detailed evaluation of the pathways and kinetics of multistep processes [8–11]. Cryogenic electron microscopy (cryo-EM) now enables structural assessment of ribosomal complexes stalled at various points during initiation with near-atomic

Figure 1

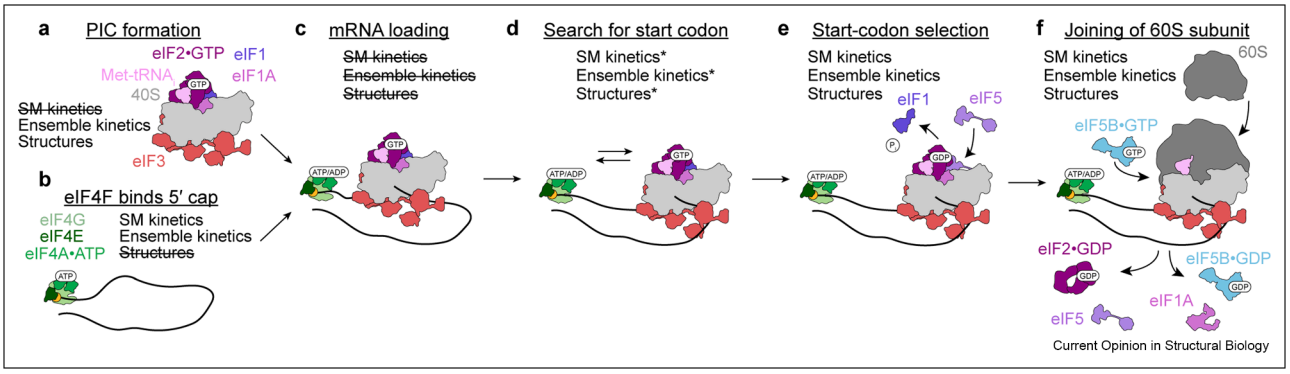

Overview of steps in canonical eukaryotic translation initiation. (a) In the first steps of initiation, several eukaryotic initiation factors (eIFs) bind the ribosomal small (40S) subunit to form a pre-initiation complex (PIC). **(b)** In parallel, the eIF4F factors assemble at the 5′ 7-methylguanine cap of the mRNA. **(c)** Interactions between eIF4F and the PIC promote loading of the mRNA into the PIC, **(d)** which is followed by a one-dimensional search along the 5′ untranslated region (UTR) of the mRNA for the start codon. **(e)** Recognition of the start codon triggers dissociation of eIF1, binding of the GTPase-activating protein eIF5, GTP hydrolysis by eIF2·GTP, and release of inorganic phosphate (P_i) from eIF2·GDP to promote full accommodation of the initiator tRNA (Met-$tRNA_i$) into the 40S subunit peptidyl-tRNA binding (P) site. **(f)** Subsequently, eIF5B·GTP binds the PIC and catalyzes subunit joining, during which several eIFs dissociate from the PIC. Whether single-molecule kinetics, ensemble kinetics, and/or structural methods have been used to directly probe individual states or steps is denoted in writing. *Kinetic data for the start codon search reports on the time delay between mRNA loading and start codon proximity rather than the time-dependent position of the PIC, and structures of this stage correspond to stalled intermediate states in the process.

resolution [12–14]. Furthermore, improvements in computational power, coarse-grained models, and enhanced sampling approaches are enabling molecular dynamics (MD) simulations to be applied to specific steps of translation [15–18].

Using the established reconstituted systems, single-molecule fluorescence measurements have probed the kinetics of certain steps in the canonical initiation process[11,19–25], and cryo-EM has been used to determine the structures of PICs representing select states in the process [13,14,26–32]. Kinetic and structural studies in yeast and mammalian systems suggest several mechanistic differences yet confirming these distinctions and elucidating their molecular basis remains challenging. In addition, the investigations conducted to date have not yet reached the levels of physical and molecular insight achieved in studies of bacterial translation or, more generally, other biological processes. These gaps in understanding persist not merely because of technical barriers but also because the focus in the field has shifted away from comprehensive investigations of the canonical initiation pathway and instead toward exploration of novel regulatory factors and their mechanisms. Here, we identify the key mechanistic gaps that remain and outline a path toward a time-dependent, molecular description of eukaryotic translation initiation grounded in advances in single-molecule fluorescence microscopy and its integration with structural methods and MD simulations.

Single-molecule fluorescence studies have partially revealed the time-dependent formation of the eIF4F complex at the cap and the composition of the PIC

Nearly all single-molecule fluorescence studies of eukaryotic translation initiation to date have probed either the time-dependent formation of the eIF4F complex at the 5′ cap of the mRNA or composition of the PIC (Figure 2) [11,19–25]. These studies have employed total internal reflection fluorescence microscopy, where binding of fluorophore-labeled components to the mRNA or PIC is detected via multi-wavelength colocalization or single-molecule fluorescence resonance energy transfer (smFRET) between two components [8,11]. Recent smFRET measurements using reconstituted yeast components indicate that eIF4G and eIF4E act as an eIF4G·E complex that can bind to one of many locations on an mRNA and diffuse along the transcript in search of the cap. At cap-distal sites, ATP-bound eIF4A promotes dissociation of eIF4G·E, thereby biasing the complex toward the 5′ end. At cap-proximal positions, however, engagement of the cap by eIF4E renders the complex resistant to this eIF4A-driven dissociation, likely because cap binding alters interactions within eIF4F in a way that inhibits eIF4A's activity. This produces a uniquely stabilized, cap-bound eIF4F complex (Figure 2a,b) [11]. Nonetheless, alternative models for the role of eIF4A in cap recognition have been inferred from smFRET studies in the yeast and mammalian systems [19,21]. It remains unclear whether the discrepancies between these

Figure 2

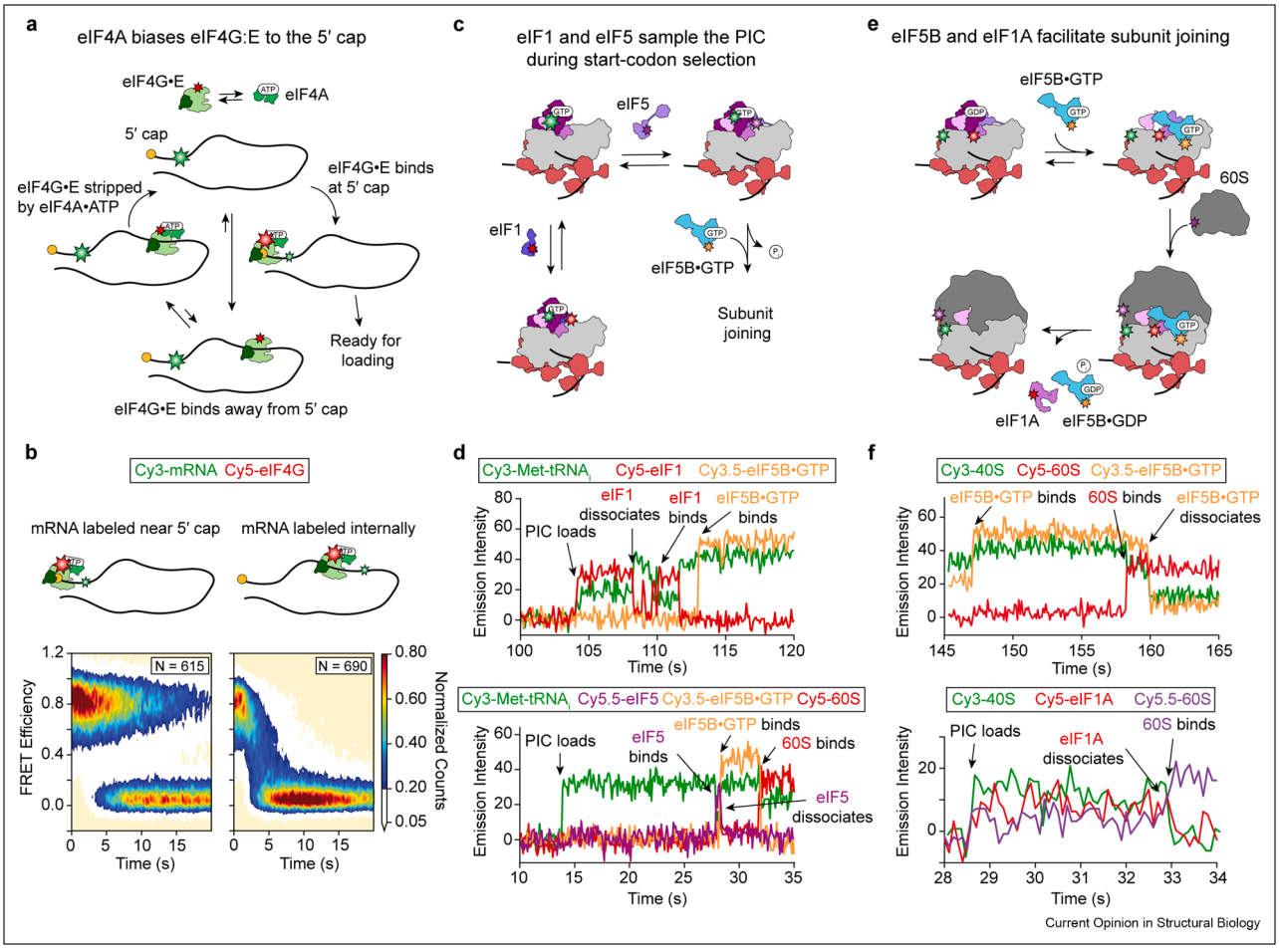

Steps of canonical eukaryotic translation initiation probed with single-molecule fluorescence microscopy. (a) smFRET signals between the mRNA and eIF4G or eIF4E in a reconstituted yeast system reveal the mechanism by which eIF4G·E is biased toward the 5′ cap by eIF4A. **(b)** Aggregate data over N trajectories for experiments where eIF4A·ATP is injected into a sample containing eIF4G·E bound to mRNA labeled near the 5′ cap or 92 nucleotides away from the cap. Detected as a loss of FRET, eIF4A·ATP facilitates >10-fold faster dissociation of eIF4G·E from internal vs. cap-proximal binding sites. **(c)** smFRET signals between Met-tRNA$_i$ and eIF1 or eIF5 in a reconstituted human system report on their competitive binding to the PIC during start codon selection. **(d)** Example fluorescence emission intensity vs. time trajectories showing (top) multiple binding and dissociation events by eIF1 before binding by eIF5B·GTP to the PIC and (bottom) binding and dissociation of eIF5 and binding by eIF5B·GTP before 60S subunit joining. **(e)** Colocalization and smFRET signals have informed on the pathways in which eIFs bind to and dissociate from the PIC during subunit joining. **(f)** Example trajectories from a reconstituted human system showing (top) binding and dissociation of eIF5B via colocalization and its timing relative to 60S subunit joining and (bottom) dissociation of eIF1A and joining of the 60S subunit via colocalization. Panels **(b)**, **(d)**, and **(f)** are adapted from Refs. [11,24], and [22], respectively. FRET, fluorescence resonance energy transfer; PIC, pre-initiation complex.

models arise from differences in the design of the smFRET experiments across studies or from non-conserved behavior of eIF4F in yeast and humans.

The time-dependent composition of the PIC has been best characterized during start codon recognition and subunit joining, where sequences of binding and dissociation by eIF1, eIF5, eIF1A, and eIF5B•GTP have been measured (Figure 2b,c) [20,22–24]. The interpretations of these data benefited from ensemble kinetics studies and several PIC cryo-EM structures determined by biochemically trapping the PICs at various stages of start codon selection or subunit joining [13,14,22,27–31,33–35]. A key observation from single-molecule trajectories of labeled PIC components is that the PIC interconverts between different compositions on millisecond-to-second timescales, even within a single stage of initiation [22–24]. For example, a study employing an smFRET signal between fluorophore-labeled Met-tRNA$_i$ and eIF1 with human components showed that eIF1 is bound to the PIC upon loading of the mRNA, dissociates from the PIC upon reaching the start codon, and subsequently transiently samples the PIC before being replaced by eIF5 (Figure 2c,d) [24]. In

the same study, an smFRET signal between Met-tRNA$_i$ and eIF5 showed that eIF5 is not bound to the PIC during mRNA loading but transiently samples the PIC when it is at the start codon [24]. During this process, eIF5 samples the PIC and outcompetes eIF1 rebinding, thereby enabling the PIC to progress toward eIF5B·GTP recruitment and 60S joining (Figure 2c,d). Beyond this, colocalization measurements of eIF1A and eIF5B have identified the pathways in which these eIFs bind to and dissociate from the PIC during subunit joining (Figure 2e,f) [22,23]. Nonetheless, factors such as eIF3, eIF2·GTP, and others have yet to be labeled and directly tracked during initiation, leaving gaps in our understanding of their time-dependent binding to and dissociation from the PIC and, consequently, their mechanisms of action during initiation.

Isolating the compositional and conformational requirements for loading of mRNA onto the PIC and scanning of the PIC along the 5′ untranslated region (UTR) remains challenging

Loading of the mRNA onto the PIC and migration of the PIC along the 5′ UTR are short-lived intermediate steps of initiation that are typically inferred indirectly from experiments and are challenging to capture in conventional structural analysis. As a result, the compositional and conformational rearrangements that the eIF4F-mRNA complex and PIC must undergo at these stages are poorly described. Long-standing questions concern (i) what interactions and conformational rearrangements of eIF4F, the mRNA, and the PIC mediate successful loading, (ii) whether eIF4F or any of its components remain bound to the mRNA or PIC after loading, and (iii) whether scanning of the PIC across the 5′ UTR occurs diffusively or in a helicase-driven fashion. Biochemical data from yeast and mammalian systems suggest that interactions between eIF4F and eIF3 (and possibly other eIFs) may be primary drivers of loading [30,36–38], but the transient interactions between eIF4F and the PIC that occur during loading have never been captured in structural studies. Competing models in which eIF4F either dissociates from the mRNA upon loading or remains bound to the mRNA or PIC arise from conflicting biochemical, structural, and ribosome profiling data [30,37,39,40]. Whether scanning occurs in a diffusive, directionally unbiased manner or via a helicase-driven, unidirectional search is still widely debated [4,20,25,30,41–43]. These models are often debated using data that report on the total duration of scanning across mRNAs with varying 5′ UTR lengths [25,42,43]. Recently, the time-dependent movement of the PIC toward the start codon has been observed with smFRET [25], but trajectory-based measurements of PIC movements across the entire 5′ UTR are needed to test the different scanning models more directly.

These studies demonstrate a need for single-molecule measurements that isolate the composition and conformations of eIF4F and the PIC during mRNA loading and scanning. Tracking of fluorophore-labeled eIF4E, eIF4G, or eIF4A has been achieved in multiple contexts [11,19,21,25,44] and, when coupled with labeling of 40S subunit- or PIC-bound eIFs, is a promising approach to reveal the status of eIF4F upon loading and scanning. smFRET signals between eIF4E, eIF4G, and/or eIF4A and the PIC would be ideal for this purpose, and recent structural characterization of these interactions in mammalian systems may be a helpful starting point for optimization of label positions [30]. Recent advances in the spatial and temporal resolution of particle-tracking techniques may permit the direct observation of PIC movement along mRNA [45]. Moreover, additional factors, including eIF4B, Ded1 (yeast), DDX3X (mammals), and others, are thought to contribute to mRNA loading and scanning [39,46,47], yet their time-dependent binding to and dissociation from eIF4F, the mRNA, or the PIC during these processes are unknown.

Single-molecule methods can probe whether and how compositional and conformational changes are coordinated and coupled during start codon selection and subunit joining

While single-molecule and ensemble kinetics have gleaned insight into the time-dependent composition of the PIC during start codon selection and subunit joining, little is known about whether and how conformational changes of the PIC are coordinated or coupled to eIF binding and the subsequent conformational motions that facilitate the late stages of initiation. Conformational changes of the PIC are thought to discriminate near-cognate or poor-context start codons from good-context AUG start codons and prime the PIC for association with the 60S subunit. To date, most understanding of such conformational changes comes from comparing cryo-EM structures stalled at different stages of initiation or from ensemble kinetics using FRET signals [13,28,33]. These studies suggest a combination of properties, including that (i) eIF1 and eIF2·GTP block complete pairing of Met-tRNA$_i$ with the codon and closure of the 40S subunit 'mRNA entry latch' via movement of the 40S subunit 'head' domain, (ii) recognition of the start codon somehow triggers reorientation of eIF1 relative to eIF1A, subsequent dissociation of eIF1 from the PIC, and repositioning of the C-terminal region of eIF1A toward eIF5, (iii) eIF5-induced GTP hydrolysis of eIF2·GTP and inorganic phosphate (P$_i$) release from eIF2·GDP·P$_i$ enables full binding of Met-tRNA$_i$ in the 40S subunit peptidyl-tRNA binding (P) site, and (iv) binding of eIF5B·GTP triggers transfer of Met-tRNA$_i$ from eIF2·GDP to eIF5B·GTP.

Structural studies have identified the start and end states of start codon selection and subunit joining as well as a limited set of intermediate states. Yet static structures cannot, on their own, establish whether these intermediates are obligatory on-pathway species or rare off-pathway conformations, underscoring the need for time-resolved approaches. Specifically, trajectory-based measurements are needed to measure the microscopic pathways of the associated conformational rearrangements. These pathways encompass both the sequences and lifetimes of conformational states as well as the short-lived trajectories in which they interconvert, known as transition paths. Transition paths contain the series of molecular configurations for an individual binding process or conformational change and they have been probed experimentally in model protein and nucleic acid systems [9]. Transition paths have yet to be experimentally probed for any step of translation initiation. Here, we focus on questions involving the sequence of occupied conformational states.

One example concerns the early changes in the PIC that facilitate switching from scanning to arrest at a start codon. This process is typically described as an equilibrium between 'open' and 'closed' PIC conformations that involves movement of Met-tRNA$_i$ in and out of the P site, tilting of the 40S subunit 'head' domain, and additional movements of, at minimum, eIF1, eIF1A, and eIF2·GTP before the initial dissociation of eIF1 (Figure 3a) [13,26,28]. Structures of the 'open' and 'closed' PIC conformations are continuously refined but the kinetics and energetics of these movements and whether and how they are modulated, coordinated, and/or coupled to discriminate the correct start codon are not clear.

In an example from Petrychenko et al. using reconstituted human factors (Figure 3b), once P$_i$ is released from eIF2·GDP·P$_i$ and the PIC commits to the start codon, cryo-EM reveals multiple distinct PIC conformations that are presumed intermediates in the subunit-joining reaction [13]. In one, eIF5 and

Figure 3

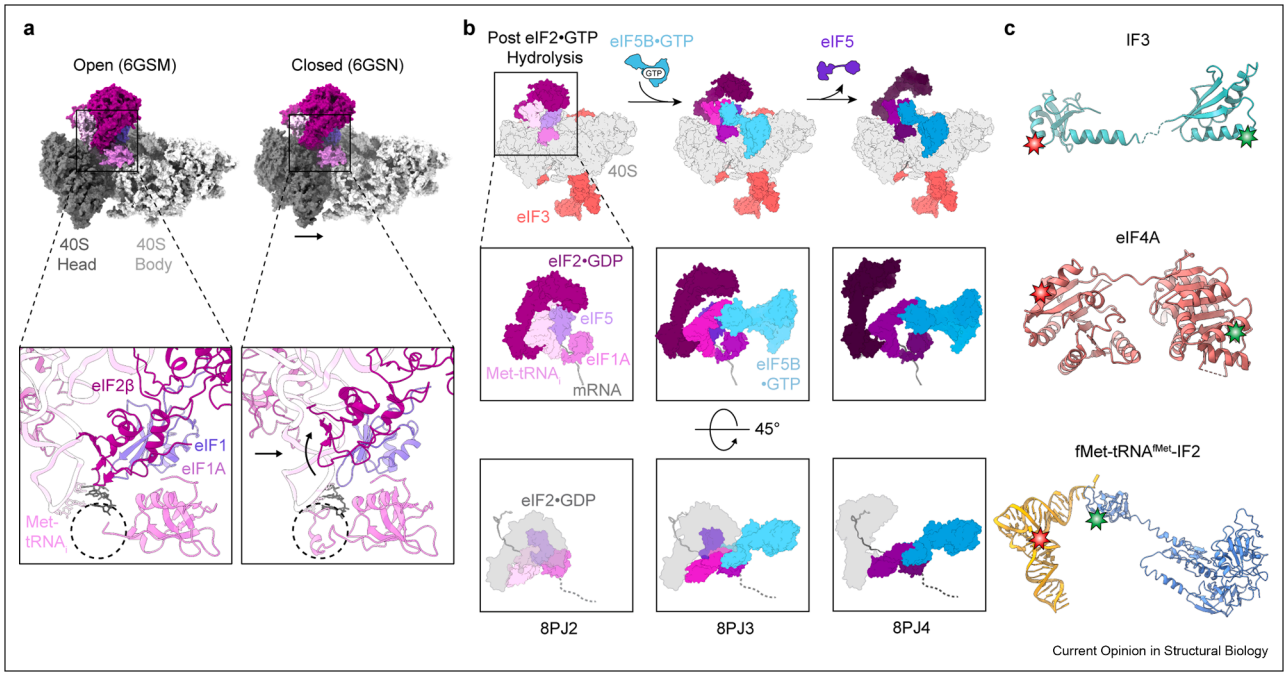

Structural snapshots and complementary single-molecule strategies for dissecting conformational changes during start codon recognition and subunit joining. (a) Cryo-EM structures of yeast PICs captured in the 'open' [PDB: 6GSM] and 'closed' [PDB: 6GSN] conformations from Llácer et al. illustrate distinct arrangements of the 40S 'head' and 'body' domains, Met-tRNA$_i$, and surrounding initiation factors (eIF3 is omitted for clarity) [28]. These snapshots suggest possible conformational transitions associated with start codon recognition, including repositioning of Met-tRNA$_i$, ordering of the eIF1A N-terminal tail (dashed circles), and altered interactions of the β subunit of eIF2 (eIF2β). Because structures capture only discrete states, their sequence, timing, and functional coupling can be established by time-resolved approaches such as smFRET. **(b)** Human PIC structures from Petrychenko et al. representing states after P$_i$ release from eIF2·GDP·P$_i$, after binding of eIF5B·GTP, and at a later stage where eIF5 appears displaced [PDBs: 8PJ2, 8PJ3, 8PJ4] provide a set of structurally inferred intermediates along the subunit-joining pathway [13]. smFRET measurements are uniquely suited to determine which of these intermediates are on pathway, how rapidly they interconvert, and how factor binding, release, and tRNA movement are coordinated in real time. **(c)** Representative fluorophore-labeled constructs developed to probe conformational changes in bacterial and eukaryotic systems using smFRET [44,49,50]. Application of analogous strategies to components of the PIC can help fill temporal and mechanistic gaps between structural snapshots illustrated in panels (a) and (b).

eIF5B·GTP are bound to the PIC, and the β and γ subunits of eIF2 (eIF2βγ) are displaced from the Met-tRNA$_i$. In another, eIF5 is unresolved and eIF2βγ are further displaced from the Met-tRNA$_i$. Nonetheless, it remains unclear whether these conformations correspond to on-pathway intermediates along a single subunit-joining pathway, on-pathway intermediates along parallel subunit-joining pathways, or off-pathway states unrelated to productive subunit joining. smFRET experiments that monitor the movement of these eIFs and/or the Met-tRNA$_i$ are well suited to resolve the conformational pathways of the PIC before subunit joining.

Moving forward, single-molecule experiments must be designed to follow new reaction coordinates sensitive to the conformational motions of the PIC. Certain strategies may be adopted from studies of bacterial translation, in which conformational changes of initiation factors have been measured directly [48—50]. These studies have utilized intermolecular smFRET signals between factors that are stably bound to the PIC or intramolecular smFRET signals where a single, PIC-bound factor is dual-labeled (Figure 3c). Similar approaches can be applied to eIFs as demonstrated by ensemble FRET signals developed between eIF1 and eIF1A, between eIF5 and eIF1A, and an smFRET signal between the RecA domains of eIF4A (Figure 3c) [33,44]. Signals that report on rearrangements of the small subunit, particularly between the 'head' and 'body' domains, are also desirable, but generating site-specific, dual-labeled small subunits, whether bacterial or eukaryotic, remains challenging.

Determining whether and how the numerous binding and dissociation reactions during initiation are mechanistically coordinated or coupled to specific structural rearrangements of the eIF4F complex and/or the PIC will likely require simultaneous monitoring of smFRET signals that report on both binding interactions and structural changes. Such measurements can be achieved with three or more distinct fluorophores such that binding/dissociation is observed via colocalization or FRET between one set of fluorophores and a conformational change is detected using an intramolecular FRET pair [51,52]. Although not yet applied to translation initiation, single-molecule tools are being developed that allow detection of time-dependent composition, conformation, and/or chemical state with subsecond to submillisecond time resolution via a combination of fluorescent readouts and non-fluorescent readouts, the latter including interferometric light scattering, particle translational diffusion, and particle charge [53—56]. Given the large molecular volumes of the 40S subunit and several eIFs, scattering and/or diffusion readouts may be ideal for probing PIC composition while simultaneously monitoring conformational changes by FRET.

Integrating single-molecule microscopy with structural biology and molecular simulations to achieve atomic-level descriptions of conformational dynamics

Single-molecule experiments will continue to be limited in the variety of reaction coordinates they can investigate. Therefore, it is essential to combine single-molecule kinetics and experimentally determined structures with MD simulations to achieve a mechanistic understanding of eukaryotic translation initiation that is detailed enough to form predictive hypotheses about how perturbations, such as mutations, regulatory factors, or drugs, influence the initiation pathway. MD simulations are essentially computational single-molecule experiments that follow time trajectories of the positions of all atoms or collective particles in a coarse-grained representation. When properly validated, MD simulations can fill in the gaps between single-molecule and structural experiments. For example, they can follow the time-dependent behavior of local interactions between substrates or with solvent molecules that are missed in trajectory-based single-molecule experiments or in structures determined by cryo-EM, characterize transition paths between conformational states, and evaluate the structural ensembles that underlie dynamic structural domains that are typically unresolved in experimentally determined structures.

Tandem application of single-molecule and structural approaches is readily achieved for eukaryotic translation initiation [22,29] but their integration with MD simulations remains largely aspirational due to poor overlap in the processes and timescales accessible by each approach. The hierarchy of structural motions and the massive size of ribosomal subunits and eIFs pose challenges for adequately sampling conformational transitions in MD simulations [15], and inaccuracies in nucleic acid force fields raise concerns about interpreting results [57]. As a result, MD simulations of processes in translation have been limited in their application and nearly all studies have focused on tRNA accommodation, intersubunit rotation, or translocation in bacterial systems [16—18,58—61]. Only recently have a few processes in eukaryotic translation been simulated [62—65]. Regardless, explicit-solvent, all-atom simulations of bacterial and eukaryotic ribosomes are typically limited to timescales of a few microseconds—orders of magnitude shorter than the timescales accessed with corresponding single-molecule investigations—and often utilize some form of enhanced sampling between free-energy minima or implementation of constraints along specified collective variables. Recent improvements in computing power, however, may eventually relax these constraints [15,66]. To address this timescale limitation in a different manner, several studies have performed MD simulations with structure-based models that can access longer timescales and can be

Figure 4

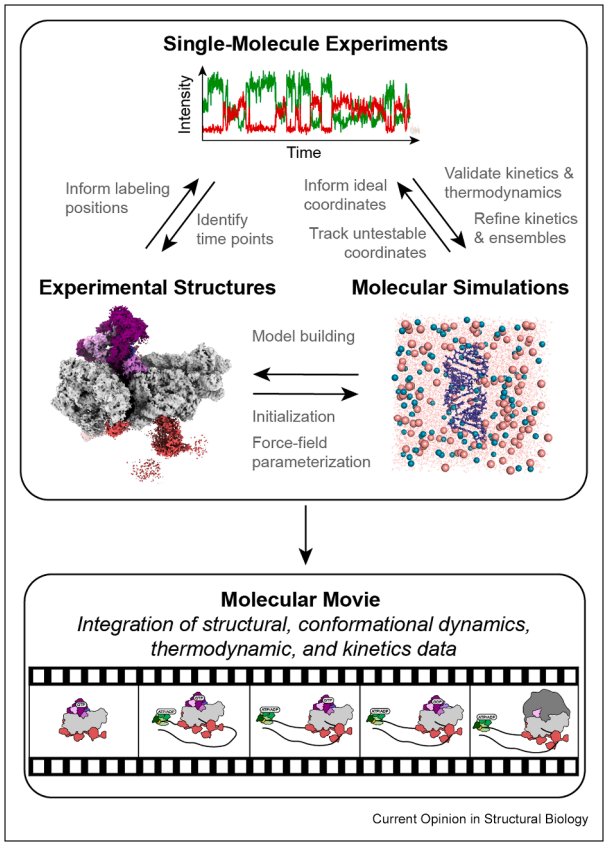

Integration of single-molecule fluorescence, experimental structural biology, and molecular simulations. Forward and backward arrows indicate that the development of each approach depends upon advances in the others. Examples by which one approach benefits another are listed next to each arrow. In some cases, one approach is needed to validate the results of another, such as when thermodynamic and kinetic parameters from MD simulations are benchmarked against single-molecule data. Alternatively, the output of one approach can directly input into another. For example, cryo-EM structures are used to initialize MD simulations of the ribosome and the thermodynamic output of MD simulations may be directly refined by experimental input. Integration of the three methodologies enables generation of a molecular movie of eukaryotic translation initiation that is rooted in accurate structural, conformational dynamics, thermodynamic, and kinetics data.

directly tuned with experimental inputs [60]. In these models, experimental structures are assumed to represent free-energy minima associated with a conformational change and are therefore used to define stabilizing interactions in the system. Such models have been applied to the few steps in bacterial and eukaryotic translation for which multiple free-energy minima are supported by a set of experimental structures, such as tRNA accommodation, translocation, and intersubunit rotation [16,60,61,64,67,68].

All MD simulations of the ribosome rely on experimental structures for initialization and/or defining free-energy minima of a conformational change; therefore, applications to eukaryotic initiation in the short term should focus on steps with sufficient structural data. Potential targets include the equilibrium between open and closed PIC conformations, comparison of Met-tRNA$_i$ and its surroundings before and after P$_i$ release from eIF2·GDP·P$_i$, transfer of Met-tRNA$_i$ from eIF2·GDP to eIF5B·GTP, and comparison of 80S ribosome-bound eIF5B before and after GTP hydrolysis. Simulations of rearrangements during mRNA loading or the binding and dissociation of eIFs from the PIC will be more challenging due to the lack of structural data and computational cost, respectively.

Deliberate and systematic integration of single-molecule measurements, structural data, and molecular simulations is necessary because each approach offers distinct molecular insight, suffers from different limitations, and depends on the others for advancement (Figure 4). Single-molecule experiments directly reveal sequences of binding interactions and conformational changes but are limited to probing movement over nanometer or larger distances and are often constrained to a time resolution of milliseconds or longer. Cryo-EM visualizes structures with high resolution but only resolves snapshots of stable conformations. MD simulations provide unmatched molecular detail and temporal resolution but suffer from their accessible time window and by questions of accuracy. MD simulations rely on high-resolution experimental structures to initialize simulations, build coarse-grained models, and refine force field parameters, particularly for nucleic acids and protein-nucleic acid complexes [60,69]. MD simulations can also leverage time-resolved experiments to validate simulated thermodynamic and kinetic properties, refine conformational ensembles and kinetics, and directly constrain the kinetics and thermodynamics of the simulation [69–73]. In turn, simulations help build and refine structural models from cryo-EM potential maps, identify the smFRET signals most sensitive to critical conformational transitions, and increasingly enable 'forward' or 'explicit' model-based comparisons between simulated and experimentally determined time trajectories [67,68,70,74–76]. Already, structural and single-molecule experiments are being used together so that structures guide the optimal placement of smFRET labels, and smFRET-derived kinetics help determine the ideal time points for time-resolved cryo-EM experiments [22,29,77]. These successes demonstrate the practical power of integrative approaches and offer a blueprint for deeper mechanistic discovery.

The convergence of single-molecule, structural, and MD simulation methodologies is rapidly becoming central to developing molecularly resolved, time-dependent descriptions of complex biological processes [69,78]. With continued advances in labeling strategies, temporal resolution, experimental

throughput, force field accuracy, and simulation strategies, the field is now poised to move beyond assembling the fragmented snapshots provided by each method in isolation toward building predictive, quantitatively grounded models of how interactions and conformational changes are coordinated to drive initiation. Realizing this vision will require sustained collaboration across disciplines but it promises to transform our understanding of eukaryotic translation initiation from a sequence of inferred steps into a coherent, mechanistically explicit, and truly dynamic molecular process.

Declaration of competing interest

There are no competing interests to disclose.

Acknowledgements

This work was supported by funds to R.L.G. from the NIH (R01 CA277727 and R35 GM153724). B.A. was supported by funds from a Helen Hay Whitney Postdoctoral Fellowship. V.S. was supported by funds from an NSF Graduate Research Fellowship (DGE − 2437839). We thank Christopher Lapointe for providing the original files used for Figure 2d,f.

References

Papers of particular interest, published within the period of review, have been highlighted as:

* of special interest
** of outstanding interest

1. Dever TE, Kinzy TG, Pavitt GD: **Mechanism and Regulation of protein synthesis in *Saccharomyces cerevisiae***. *Genetics* 2016, **203**:65–107.

2. Shivaya Valasek L: **'Ribozoomin' – translation initiation from the perspective of the ribosome-bound eukaryotic initiation factors (eIFs)**. *Curr Protein Pept Sci* 2012, **13**:305–330.

3. Acker MG, Kolitz SE, Mitchell SF, Nanda JS, Lorsch JR: **Reconstitution of yeast translation initiation**. *Methods Enzymol* 2007, **430**:111–145.

4. Pestova TV, Kolupaeva VG: **The roles of individual eukaryotic translation initiation factors in ribosomal scanning and initiation codon selection**. *Genes Dev* 2002, **16**:2906–2922.

5. Mitchell SF, Walker SE, Algire MA, Park EH, Hinnebusch AG, Lorsch JR: **The 5'-7-methylguanosine cap on eukaryotic mRNAs serves both to stimulate canonical translation initiation and to block an alternative pathway**. *Mol Cell* 2010, **39**: 950–962.

6. Hinnebusch AG: **The scanning mechanism of eukaryotic translation initiation**. *Annu Rev Biochem* 2014, **83**:779–812.

7. Merrick WC, Pavitt GD: **Protein synthesis initiation in eukaryotic cells**. *Cold Spring Harbor Perspect Biol* 2018, **10**: a033092.

8. Chen J, Dalal RV, Petrov AN, Tsai A, O'Leary SE, Chapin K, Cheng J, Ewan M, Hsiung P-L, Lundquist P, *et al.*: **High-throughput platform for real-time monitoring of biological processes by multicolor single-molecule fluorescence**. *Proc Natl Acad Sci USA* 2014, **111**:664–669.

9. Chung HS: **Transition path times measured by single-molecule spectroscopy**. *J Mol Biol* 2018, **430**:409–423.

10. Lerner E, Barth A, Hendrix J, Ambrose B, Birkedal V, Blanchard SC, Börner R, Chung HS, Cordes T, Craggs TD, *et al.*: **FRET-based dynamic structural biology: challenges, perspectives and an appeal for open-science practices**. *eLife* 2021, **10**, e60416.

11. ** Gentry RC, Ide NA, Comunale VM, Hartwick EW, Kinz-Thompson CD, Gonzalez RL: **The mechanism of mRNA cap recognition**. *Nature* 2024, **637**:736–743.
Using smFRET on full-length mRNAs, this study shows that yeast eIF4G·E can bind to one of many locations on an mRNA and diffuse along the transcript in search of the cap. ATP-bound eIF4A promotes dissociation of eIF4G·E from non-productive, cap-distal sites, while cap-bound eIF4E allosterically blocks this dissociation activity, selectively stabilizing eIF4G·E·A (eIF4F) at the cap. The selective stabilization of an eIF4F complex at the cap defines an 'activated' mRNA that can recruit a PIC.

12. Korostelev AA: **The structural dynamics of translation**. *Annu Rev Biochem* 2022, **91**:245–267.

13. * Petrychenko V, Yi S-H, Liedtke D, Peng B-Z, Rodnina MV, Fischer N: **Structural basis for translational control by the human 48S initiation complex**. *Nat Struct Mol Biol* 2024, **32**: 62–72.
Using cryo-EM, this study resolved structures of reconstituted human PICs that presumably represent intermediates along the start-codon-selection and subunit-joining pathways. The structures reveal conformational changes associated with P_i release from eIF2·GDP·P_i and show how rearrangements within eIF3 can reposition its subunits away from the intersubunit interface, thereby priming the complex for productive subunit joining.

14. Brito Querido J, Sokabe M, Kraatz S, Gordiyenko Y, Skehel JM, Fraser CS, Ramakrishnan V: **Structure of a human 48S translational initiation complex**. *Science* 2020, **369**: 1220–1227.

15. Sanbonmatsu K: **Supercomputing in the biological sciences: toward Zettascale and Yottascale simulations**. *Curr Opin Struct Biol* 2024, **88**, 102889.

16. Byju S, Hassan A, Whitford PC: **The energy landscape of the ribosome**. *Biopolymers* 2024, **115**, e23570.

17. Bock LV, Gabrielli S, Kolář MH, Grubmüller H: **Simulation of complex biomolecular systems: the ribosome challenge**. *Annu Rev Biophys* 2023, **52**:361–390.

18. ** Sanbonmatsu K, Prajapati J: **Ribosomal tRNA release decoded via multiscale simulations at biological timescales**. *Res Sq* 2025, https://doi.org/10.21203/rs.3.rs-7966662/v1.
This study developed an MD simulation approach that combined a rigid-body framework and high-temperature enhanced sampling to capture a hundred trajectories in which deacylated tRNA dissociates from the ribosomal tRNA exit (E) site of the bacterial 70S ribosome, a process observed to occur over hundreds of milliseconds to seconds in smFRET experiments. This approach marks a milestone in the ability to sample substrate dissociation from the ribosome. It is also a promising step towards simulating previously inaccessible processes in translation that occur on the timescales of seconds.

19. Çetin B, O'Leary SE: **mRNA- and factor-driven dynamic variability controls eIF4F-cap recognition for translation initiation**. *Nucleic Acids Res* 2022, **50**:8240–8261.

20. Hong HJ, Zhang AL, Conn AB, Blaha G, O'Leary SE: **Single-molecule tracking reveals dynamic regulation of ribosomal scanning**. *Sci Adv* 2024, **10**:eadm9801.

21. * Hong HJ, Guevara MG, Li S, Liu Y, Huang AN, Lin E, Neal A, Xu D, Hai R, Zandi R, *et al.*: **Dynamics and regulation of mRNA cap recognition by human eIF4F**. *bioRxiv* 2025, https://doi.org/10.1101/2025.06.26.660926.
This study used smFRET between eIF4E and an mRNA-hybridized oligonucleotide to monitor the real-time kinetics of eIF4F association with and dissociation from mRNA in a fully reconstituted human initiation system. By systematically dropping out eIFs, slowing or blocking the hydrolysis of ATP by eIF4A, and testing the effects of various mRNAs, the authors define how specific components of the human initiation machinery modulate eIF4F association and dissociation during canonical eukaryotic initiation.

22. Lapointe CP, Grosely R, Sokabe M, Alvarado C, Wang J, Montabana E, Villa N, Shin BS, Dever TE, Fraser CS, *et al.*: **eIF5B and eIF1A reorient initiator tRNA to allow ribosomal subunit joining**. *Nature* 2022, **607**:185–190.

23. Wang J, Johnson AG, Lapointe CP, Choi J, Prabhakar A, Chen D-H, Petrov AN, Puglisi JD: **eIF5B gates the transition from translation initiation to elongation**. *Nature* 2019, **573**: 605–608.

24. ** Grosely R, Alvarado C, Ivanov IP, Nicholson OB, Puglisi JD, Dever TE, Lapointe CP: **eIF1 and eIF5 dynamically control translation start site fidelity**. *Nat Struct Mol Biol* 2025, **32**: 2308–2318.

This study used smFRET with reconstituted human PICs to observe how eIF1 and eIF5 bind to and dissociate from the PIC at cognate vs. near-cognate start codons. By monitoring FRET signals between labeled Met-tRNA$_i$ and eIF1 or eIF5, the authors conclude that eIF1 initially binds the PIC prior to mRNA loading and then transiently rebinds after start-site recognition, whereas eIF5 binds in a competing manner that terminates eIF1 rebinding and drives commitment to initiation. The kinetics of both factors are differentially modulated on near-cognate start codons, consistent with a model in which their dynamic interplay tunes start-site fidelity.

25. Wang J, Shin BS, Alvarado C, Kim JR, Bohlen J, Dever TE, Puglisi JD: **Rapid 40S scanning and its regulation by mRNA structure during eukaryotic translation initiation**. *Cell* 2022, **185**:4474–4487.

26. Llácer JL, Hussain T, Marler L, Aitken CE, Thakur A, Lorsch JR, Hinnebusch AG, Ramakrishnan V: **Conformational differences between open and closed states of the eukaryotic translation initiation complex**. *Mol Cell* 2015, **59**:399–412.

27. Llácer JL, Hussain T, Saini AK, Nanda JS, Kaur S, Gordiyenko Y, Kumar R, Hinnebusch AG, Lorsch JR, Ramakrishnan V: **Translational initiation factor eIF5 replaces eIF1 on the 40S ribosomal subunit to promote start-codon recognition**. *eLife* 2018, **7**, e39273.

28. Llácer JL, Hussain T, Dong J, Villamayor L, Gordiyenko Y, Hinnebusch AG: **Large-scale movement of eIF3 domains during translation initiation modulate start codon selection**. *Nucleic Acids Res* 2021, **49**:11491–11511.

29. Wang J, Wang J, Shin B-S, Kim J-R, Dever TE, Puglisi JD, Fernández IS: **Structural basis for the transition from translation initiation to elongation by an 80S-eIF5B complex**. *Nat Commun* 2020, **11**:5003.

30. * Brito Querido J, Sokabe M, Díaz-López I, Gordiyenko Y, Fraser CS, Ramakrishnan V: **The structure of a human translation initiation complex reveals two independent roles for the helicase eIF4A**. *Nat Struct Mol Biol* 2024, **31**:455–464.

Using cryo-EM, this study reconstructed three-dimensional electrostatic potential maps of reconstituted human PICs that include density the authors interpreted as eIF4G together with two copies of eIF4A, one positioned within eIF4F near the mRNA entry channel and the other positioned near the mRNA exit channel. The structures also show eIF4F in contact with both eIF3 and the 40S subunit. Based on these features, the authors propose that eIF4A plays two mechanistically distinct roles, one during mRNA recruitment and another during scanning.

31. Yi S-H, Petrychenko V, Schliep JE, Goyal A, Linden A, Chari A, Urlaub H, Stark H, Rodnina MV, Adio S, *et al.*: **Conformational rearrangements upon start codon recognition in human 48S translation initiation complex**. *Nucleic Acids Res* 2022, **50**: 5282–5298.

32. Bochler A, Querido JB, Prilepskaja T, Soufari H, Simonetti A, Del Cistia ML, Kuhn L, Ribeiro AR, Valášek LS, Hashem Y: **Structural differences in translation initiation between pathogenic trypanosomatids and their mammalian hosts**. *Cell Rep* 2020, **33**, 108534.

33. Nanda JS, Saini AK, Muñoz AM, Hinnebusch AG, Lorsch JR: **Coordinated movements of eukaryotic translation initiation factors eIF1, eIF1A, and eIF5 trigger phosphate release from eIF2 in response to start codon recognition by the ribosomal preinitiation complex***. *J Biol Chem* 2013, **288**:5316–5329.

34. Acker MG, Shin B-S, Nanda JS, Saini AK, Dever TE, Lorsch JR: **Kinetic analysis of late steps of eukaryotic translation initiation**. *J Mol Biol* 2009, **385**:491–506.

35. Villamayor-Belinchón L, Sharma P, Gordiyenko Y, Llácer JL, Hussain T: **Structural basis of AUC codon discrimination during translation initiation in yeast**. *Nucleic Acids Res* 2024, **52**:11317–11335.

36. Yourik P, Aitken CE, Zhou F, Gupta N, Hinnebusch AG, Lorsch JR: **Yeast eIF4A enhances recruitment of mRNAs regardless of their structural complexity**. *eLife* 2017, **6**, e31476.

37. Kumar P, Hellen CUT, Pestova TV: **Toward the mechanism of eIF4F-mediated ribosomal attachment to mammalian capped mRNAs**. *Genes Dev* 2016, **30**:1573–1588.

38. Villa N, Do A, Hershey JWB, Fraser CS: **Human eukaryotic initiation factor 4G (eIF4G) protein binds to eIF3c, -d, and -e to promote mRNA recruitment to the ribosome**. *J Biol Chem* 2013, **288**:32932–32940.

39. Pelletier J, Sonenberg N: **The organizing principles of eukaryotic ribosome recruitment**. *Annu Rev Biochem* 2019, **88**:307–335.

40. Bohlen J, Fenzl K, Kramer G, Bukau B, Teleman AA: **Selective 40S footprinting reveals cap-tethered ribosome scanning in human cells**. *Mol Cell* 2020, **79**:561–574.

41. Wakabayashi H, Zhu M, Grayhack EJ, Mathews DH, Ermolenko DN: **40S ribosomal subunits scan mRNA for the start codon by one-dimensional diffusion**. *RNA* 2025, **31**: 1488–1502.

42. Vassilenko KS, Alekhina OM, Dmitriev SE, Shatsky IN, Spirin AS: **Unidirectional constant rate motion of the ribosomal scanning particle during eukaryotic translation initiation**. *Nucleic Acids Res* 2011, **39**:5555–5567.

43. Berthelot K, Muldoon M, Rajkowitsch L, Hughes J, McCarthy JEG: **Dynamics and processivity of 40S ribosome scanning on mRNA in yeast**. *Mol Microbiol* 2004, **51**: 987–1001.

44. Harms U, Andreou AZ, Gubaev A, Klostermeier D: **eIF4B, eIF4G and RNA regulate eIF4A activity in translation initiation by modulating the eIF4A conformational cycle**. *Nucleic Acids Res* 2014, **42**:7911–7922.

45. Scheiderer L, Marin Z, Ries J: **MINFLUX achieves molecular resolution with minimal photons**. *Nat Photonics* 2025, **19**: 238–247.

46. Walker SE, Zhou F, Mitchell SF, Larson VS, Valasek L, Hinnebusch AG, Lorsch JR: **Yeast eIF4B binds to the head of the 40S ribosomal subunit and promotes mRNA recruitment through its N-terminal and internal repeat domains**. *RNA* 2013, **19**:191–207.

47. Gupta N, Lorsch JR, Hinnebusch AG: **Yeast Ded1 promotes 48S translation pre-initiation complex assembly in an mRNA-specific and eIF4F-dependent manner**. *eLife* 2018, **7**, e38892.

48. Lai W-JC, Ermolenko DN: **Ensemble and single-molecule FRET studies of protein synthesis**. *Methods* 2018, **137**:37–48.

49. Elvekrog MM, Gonzalez RL: **Conformational selection of translation initiation factor 3 signals proper substrate selection**. *Nat Struct Mol Biol* 2013, **20**:628–633.

50. Caban K, Pavlov M, Ehrenberg M, Gonzalez RL: **A conformational switch in initiation factor 2 controls the fidelity of translation initiation in bacteria**. *Nat Commun* 2017, **8**:1475.

51. Bilgen E, Lamb DC: **Multicolor single-molecule FRET studies on dynamic protein systems**. *Curr Opin Struct Biol* 2025, **93**, 103117.

52. Feng XA, Poyton MF, Ha T: **Multicolor single-molecule FRET for DNA and RNA processes**. *Curr Opin Struct Biol* 2021, **70**: 26–33.

53. Ortega Arroyo J, Cole D, Kukura P: **Interferometric scattering microscopy and its combination with single-molecule fluorescence imaging**. *Nat Protoc* 2016, **11**:617–633.

54. Carpenter WB, Lavania AA, Squires AH, Moerner WE: **Label-Free anti-brownian trapping of single nanoparticles in solution**. *J Phys Chem C* 2024, **128**:20275–20286.

55. Wilson H, Wang Q: **ABEL-FRET: tether-free single-molecule FRET with hydrodynamic profiling**. *Nat Methods* 2021, **18**: 816–820.

56. Wang Q: **Electrokinetic detection of single-molecule phosphorylation**. *J Am Chem Soc* 2025, **147**:21308–21312.

57. Šponer J, Bussi G, Krepl M, Banáš P, Bottaro S, Cunha RA, Gil-Ley A, Pinamonti G, Poblete S, Jurečka P, *et al.*: **RNA structural dynamics as captured by molecular simulations: a comprehensive overview**. *Chem Rev* 2018, **118**:4177–4338.

58. Whitford PC, Onuchic JN, Sanbonmatsu KY: **Connecting energy landscapes with experimental rates for Aminoacyl-tRNA accommodation in the ribosome**. *J Am Chem Soc* 2010, **132**:13170–13171.

59. Warias M, Grubmüller H, Bock LV: **tRNA dissociation from EF-Tu after GTP hydrolysis: primary steps and antibiotic inhibition**. *Biophys J* 2020, **118**:151–161.

60. Levi M, Noel JK, Whitford PC: **Studying ribosome dynamics with simplified models**. *Methods* 2019, **162–163**:128–140.

61. Nishima W, Girodat D, Holm M, Rundlet EJ, Alejo JL, Fischer K, Blanchard SC, Sanbonmatsu KY: **Hyper-swivel head domain motions are required for complete mRNA-tRNA translocation and ribosome resetting**. *Nucleic Acids Res* 2022, **50**: 8302–8320.

62. Lind C, Åqvist J: **Principles of start codon recognition in eukaryotic translation initiation**. *Nucleic Acids Res* 2016, **44**: 8425–8432.

63. * Wanes G, Mohanty U, Whitford P: **Transient ion-mediated interactions regulate subunit rotation in a eukaryotic ribosome**. *bioRxiv* 2025, https://doi.org/10.1101/2025.08.09.669508.
This work developed a structure-based model of the yeast 80S ribosome that explicitly includes both inner-shell and diffuse ions. Using this model, the authors performed MD simulations that describe how Mg^{2+} concentration modulates the conformational free-energy landscape of the ribosome, revealing that transient ion-mediated interactions help regulate transitions between non-rotated and rotated states of the ribosome.

64. ** Sapkota D, Sanbonmatsu KY, Girodat D: **Human protein synthesis requires aminoacyl-tRNA pivoting during proofreading**. *Nat Commun* 2025, **16**:8202.
This study used MD simulations with structure-based models of the *Escherichia coli* and human ribosomes to compare the energetics and dynamics of aminoacyl-tRNA (aa-tRNA) accommodation into the ribosomal aa-tRNA binding (A) site. The simulations suggest that human aa-tRNA undergoes a characteristic pivoting motion as it accommodates into the A site, and that this motion introduces an additional energetic barrier not present in bacteria. These findings provide a molecular explanation for the ~10-fold slower accommodation rate observed in human reconstituted systems relative to bacterial ribosomes.

65. Kameda T, Asano K, Togashi Y: **Free energy landscape of RNA binding dynamics in start codon recognition by eukaryotic ribosomal pre-initiation complex**. *PLoS Comput Biol* 2021, **17**, e1009068.

66. Shaw DE, Adams PJ, Azaria A, Bank JA, Batson B, Bell A, Bergdorf M, Bhatt J, Butts JA, Correia T, *et al.*: **Anton 3: twenty microseconds of molecular dynamics simulation before lunch**. In *Proceedings of the international conference for high performance computing, networking, storage and analysis*; 2021:1–11.

67. Hassan A, Whitford PC: **Identifying strategies to experimentally probe multidimensional dynamics in the ribosome**. *J Phys Chem B* 2022, **126**:8460–8471.

68. Noel JK, Chahine J, Leite VBP, Whitford PC: **Capturing transition paths and transition states for conformational rearrangements in the ribosome**. *Biophys J* 2014, **107**:2881–2890.

69. Bernetti M, Bussi G: **Integrating experimental data with molecular simulations to investigate RNA structural dynamics**. *Curr Opin Struct Biol* 2023, **78**, 102503.

70. Girodat D, Pati AK, Terry DS, Blanchard SC, Sanbonmatsu KY: **Quantitative comparison between sub-millisecond time resolution single-molecule FRET measurements and 10-second molecular simulations of a biosensor protein**. *PLoS Comput Biol* 2020, **16**, e1008293.

71. Matsunaga Y, Sugita Y: **Use of single-molecule time-series data for refining conformational dynamics in molecular simulations**. *Curr Opin Struct Biol* 2020, **61**:153–159.

72. Brotzakis ZF, Vendruscolo M, Bolhuis PG: **A method of incorporating rate constants as kinetic constraints in molecular dynamics simulations**. *Proc Natl Acad Sci USA* 2021, **118**, e2012423118.

73. Leone V, Marinelli F: **From snapshots to ensembles: integrating experimental data and dynamics**. *Curr Opin Struct Biol* 2025, **95**, 103155.

74. Dodd T, Yan C, Ivanov I: **Simulation-based methods for model building and refinement in cryoelectron microscopy**. *J Chem Inf Model* 2020, **60**:2470–2483.

75. Miller JJ, Mallimadugula UL, Zimmerman MI, Stuchell-Brereton MD, Soranno A, Bowman GR: **Accounting for fast vs slow exchange in single molecule FRET experiments reveals hidden conformational states**. *J Chem Theor Comput* 2024, **20**:10339–10349.

76. Montepietra D, Tesei G, Martins JM, Kunze MBA, Best RB, Lindorff-Larsen K: **FRETpredict: a Python package for FRET efficiency predictions using rotamer libraries**. *Commun Biol* 2024, **7**:298.

77. Kaledhonkar S, Fu Z, Caban K, Li W, Chen B, Sun M, Gonzalez RL, Frank J: **Late steps in bacterial translation initiation visualized using time-resolved cryo-EM**. *Nature* 2019, **570**:400–404.

78. Pokorná P, Aupič J, Fica SM, Magistrato A: **Decoding spliceosome dynamics through computation and experiment**. *Chem Rev* 2025, **125**:9807–9833.